Celal Bayar University Journal of Science

Comparative Evaluation for PCA and ICA on Tongue-Machine Interface Using Glossokinetic Potential Responses

Kutlucan Gorur[1,*], M. Recep Bozkurt[2], M. Serdar Bascil[3], Feyzullah Temurtas[1]

[1]Department of Electrical and Electronics Engineering, Bandirma Onyedi Eylul University, 10200 Balikesir, Turkey
[2] Department of Electrical and Electronics Engineering, Sakarya University, 54187 Sakarya, Turkey
[3]Department of Electrical and Electronics Engineering, Yozgat Bozok University, 66200 Yozgat, Turkey
[*]kutlucan.gorur@yobu.edu.tr

Received: 30 May 2019
Accepted: 17 March 2020
DOI: 10.18466/cbayarfbe.571994

Abstract

The tongue-machine interface (TMI) between the paralyzed person and computer makes it possible to manage assistive technologies. Severely disabled individuals caused by traumatic brain and spinal cord injuries need continuous help to carry out everyday routines. The cranial nerve is arisen directly from the brain to connect the tongue that is one of the last affected organs in neuromuscular disorders. Besides, the tongue has highly capable of mobility located in the oral cavity, which also provides cosmetic advantages. These crucial skills make the tongue to be an odd organ employed in the human-machine interfaces. In this study, it was aimed to investigate 1-D extraction and develop a novel tongue-machine interface using the glossokinetic potential responses (GKPs). This rarely used bio-signs are occurred by contacting the buccal walls with the tip of the tongue in the oral cavity. Our study, named as GKP-based TMI measuring the glossokinetic potential responses over the scalp, may serve paralyzed persons an unobtrusive, natural, and reliable communication channel. In this work, 8 males and 2 females, aged between 22-34 naive healthy subjects, have participated. Linear discriminant analysis and support vector machine were implemented with mean-absolute value and power spectral density feature extraction process. Moreover, independent component analysis (ICA) and principal component analysis (PCA) were used to evaluate the reduced dimension of the data set for GKPs in machine learning algorithms. Furthermore, the highest result was obtained at 97.03%.

Keywords: Assistive Technologies, Glossokinetic Potential Responses, Independent Component, Analysis, Principal Component Analysis, Tongue-Machine Interface

1. Introduction

Assistive technologies (AT) are crucial to helping disabled persons with their intentions to evolve the quality of life. Individuals with spinal cord injury (SCI), locked-in syndrome (LIS), and other impairments of the degenerative neuromuscular disorders require self-supported possibilities to be able tasks in performing daily needs without another person's continuous help [1]. There are so many ongoing research on a kind of electroencephalography (EEG)-based brain-computer interfaces (BCI) developed for paralyzed persons. Other systems such as head and eye trackers demand high concentration and visual dependence. Then these systems may result in neck pains. However, tongue-operated methods are convenient because they are almost invisible and manageable. Moreover, the tongue is characterized as a good manipulator for assistive devices, including sophisticated motor control [2]. The hypoglossal cranial nerve is the bridge between the brain and tongue, which has the ability direct communication channel at a relatively low distance from the brain.

Furthermore, the tongue can not be damaged easily and named as the last affected organ in spinal cord injuries. Another advantage of using the tongue in ATs is that this organ has complex muscle groups and is not exhausted due to the less sensed effort [3-5]. Besides, the oral cavity is a very sensitive area compared to other body parts. Oral structures perform a cortex mapping similar to hand size. In contrast, the whole body and lower limbs of the body have a relatively small mapping in the somatic sensory cortex. Otherwise, some mouth structures such as the tongue are more delicate than the fingertip according to the psychophysical papers about the strength of discrimination and sensitivity [6]. For this reason, it appears that tongue can yield encouraging

performances for a human-machine interface (HMI) compared to other body parts, depending on the cortex brain mapping [7-8].

Glossokinetic potentials are electrical responses, which occur when the tongue touches the tissues in the mouth, especially the buccal walls. The tip of the tongue possesses a negative electric charge compared to the tongue root; therefore, when the tongue touches the tissues, it causes decreasing of potential levels near the contact surface. Hence analyzing the spatial pattern of GKP responses can be used to trace the tongue movements inside the mouth. GKPs originate in the noncerebral region, therefore interfering with the alpha/beta frequencies obtained from mental activities is very low. Because delta (1-3 Hz) and theta (4-7 Hz) waves occur in the low bands of frequencies [3-5]. In conventional synchronous brain-computer interfaces, the nonstationary EEG signals have inherent problems. These are the loss of control (LoC) and degrees of freedom (DoF) [9]. Besides, the major disadvantages of synchronous BCIs are shown as high cognitive workload and long training duration [10]. At this point, GKP and tongue might serve to give solutions without so much effort due to voluntary intuitive movements.

Recently, tongue-operated assistive technologies have been proposed in the literature. Few of them are benefited from the glossokinetic potentials. Nam et al. have developed the "Tongue Rudder." In this article, the researchers measured GKPs and electromyography (EMG) electrical signals over the scalp to drive the electric wheelchair for 1-D control. Then the teeth clenching is to calibrate and toggle the wheelchair [4]. The same authors have also attempted the "GOM-Face." In this work, electrooculogram (EOG) biosignals were utilized besides the GKP and EMG to remote the humanoid robot for 2-D control in a real-time application. All the potential variations were recorded from the face. Eigenvalue decomposition of two covariance was determined to discriminate eye and tongue movements due to being called charged organs. Then the SVM was employed to recognize each movement. Also, the review paper of the glossokinetic potential in using the ATs was published by the same researchers [5]. At this point, to the best of our knowledge, this research is also the first attempt using the support vector machine (SVM) and linear discriminant analysis (LDA) with power spectral density (PSD) and mean-absolute value (MV) using GKPs to structure a TMI.

So far, considerable amount of the tongue-driven work on the assistive devices has been dealing with the hardware inside the mouth and around the headset. Primary of them are; Huo et al. realized a series of tongue-driven systems that communicate with wireless transmissions in a state of stroke. Some were connected directly to the computer, and others were forwarded via smartphone for processing. However, they have a similar principle. A small permanent magnet is connected to trace the induced magnetic variations on the scheme of sensors assembled in the oral cavity [1]. Krishnamurthy et al. handled a similar principle to carry out an interface technology [11]. Nevertheless, interfaces operated by such an equipment-based system can irritate paralyzed patients while breathing or speaking, and at the same time are not hygienic and visually appealing. Therefore, GKP-based TMI may offer a natural, fast, attractive, and accurate control approach for stroke individuals.

Another approach of a tongue-based interface is on the airflow pressure variations generated by the tongue movements in the oral cavity. Vaidyanathan et al., have designed several ATs using a microphone attached to the ear canal to detect changes of airflow pressure in the ear canal due to the discrete tongue movements [12]. However, GKP-based TMI may contribute an inherent solution to trace the tongue motion without disturbing the listening performance.

This article is intended to carry out a natural, reliable, fast, and easy-to-use tongue-operated machine for stroke patients. GKP-based TMI is a novel AT utilizing glossokinetic potential responses to extract 1-D motion. The experimental paradigm has been configured in the offline measurement. Linear discriminant analysis and support vector machine and were employed in mean-absolute value (MAV) and power spectral density (PSD) methods. Moreover, principal component analysis (PCA) and independent component analysis (ICA) were implemented to the data to reduce the dimension. And comparison was made by these methods (ICA and PCA) in the article.

2. Materials and Methods

The glossokinetic potential responses were measured over the scalp in terms of the 10-20 international system for the location of electrodes [8]. The left-eyebrow and earlobes of left-right (A1-A2) were assigned as ground and reference, respectively. The monopolar placement of electrodes is represented in Table 1. The sampling frequency was at 1024 Hz and 0.5-100 Hz range was implemented for filtering operation. Also, the notch filter of 50 Hz was applied for elimination the noise of the power line. Then GKP biosignals were filtered using a low-pass filter of 10th order infinite impulse response (IIR) Butterworth in the cutoff frequency of 40 Hz [8]. The low-pass filtering EOG signal processing was also made at the same time because of the general assumption for lower frequency filtering (40 and 100 Hz) of EOG signals.

Celal Bayar University Journal of Science
Volume 16, Issue 1, 2020, p 35-46
Doi: 10.18466/cbayarfbe.571994

Table 1. The Monopolar Placement Electodes.

Number of Channels	Name of Channels
1	Fp2
2	Fp1
3	F7
4	F3
5	Fz
6	F4
7	F8
8	T3
9	C3
10	Cz
11	C4
12	T4
13	T5
14	P3
15	Pz
16	P4
17	T6
18	O1
19	O2

Then filtered data was normalized in the range of (0-1) according to the Eq.2.1 below:

$$X_S^{norm} = \frac{X_S - X_{min}}{X_{max} - X_{min}} \qquad (\mathbf{2.1})$$

X_S defines the *sth* data in the data set, X_{max} (maximum) and X_{min} (minimum) are the least and highest values [8]. The main illustration of the system can be viewed in Fig.1.

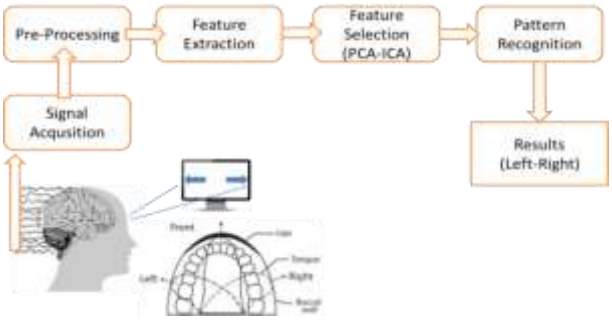

Figure 1. The workflow graph of GKP-based TMI.

2.1. Data Collection

This work consists of naive healthy subjects (8 male and 2 female) who were right-handed without any disorder of the nervous system. Subjects were in a comfortable situation placed in front of the LCD screen half-meter away without any movement except tongue movements during the experimental setup instructions. The statistical information for each participant can be shown in Table 2.

GKPs were measured and recorded by employing the EEG signal acquisition device of Micromed SAM32RFO with 19 channels, and the electrode impedances were held below 10kΩ. The recorded each trial was 98 seconds and initiated after the 10 s delay. Each touching process was 6 s, and the rest period was 5 s between the following instructions for right- left tongue movements. Four right and four left tongue movements were implemented in terms of the experimental sequences represented in Fig.2. For each channel, 6 s tongue movements and toucings to the buccal walls are stored with digitized samples of (6×1024). Participants were directed to touch the tongue and buccal walls during distinct, fast, and rhythmic contacts between 10-15 times for 6 seconds. Then, the resting time of the extended tongue was 5 seconds and no longer motion at this interval.

Table 2. Statistical information for each participant.

	Gender	Age
Subject-1	F	25
Subject-2	M	23
Subject-3	M	22
Subject-4	F	22
Subject-5	M	23
Subject-6	M	32
Subject-7	M	22
Subject-8	M	25
Subject-9	M	23
Subject-10	M	34

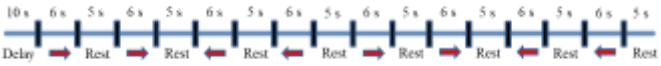

Figure 2. The experimental setup sequence of tongue Movements.

2.2. Feature Extraction

The transformation of the input signal data into a feature vector is named as feature extraction. The stage's purpose is to highlight distinctive properties in the input signal patterns. Mean-absolute value (time-domain) and power spectral density (frequency domain) methods were implemented in this research study. MAV is situated on the signal amplitude and does not need a transformation process between domains [8]. However, PSD has a transformation stage that implies more computational time. Frequency domain properties are calculated, estimating the power spectrum density of the signal and are implemented via parametric methods and periodogram [8]. In Eq.2.2, the mathematical presentation of the mean-absolute value is defined as:

$$MAV = \frac{1}{N}\sum_{i=1}^{N}|x_i| \qquad (\mathbf{2.2})$$

where X_i=1,2,3…N shows time series of samples, and N means the samples' length. Power signal variations of hemispherical scalp in motor tasks including the tongue

have different frequency ranges on the cortex that the PSD exhibits. The PSD is a function that defines the power distribution over a signal frequency. The mathematical expression of PSD is as follows in Eqs.2.3.-2.6.:

$$Px(f) = \frac{1}{N}\left|\sum_{n=0}^{N-1} x(n)e^{-j2\pi fn}\right|^2 = \frac{1}{N}|X(f)|^2 \quad (\mathbf{2.3})$$

where *X(f)* means the Fourier transform of the data sequence of *x(n)* and *N* is length of the sampled signal. The PSD formation is periodogram. Moreover the Welch's method is a special usage of periodogram. The data segments are divided and then overlapped, as shown below:

$$x_i(n) = x(n + iD) \quad n = 0,1,\dots,M-1 \quad i = 0,1,\dots,L-1 \quad \mathbf{(2.4)}$$

where *i* represents the segment of the data, while *n* is the segment length. Moreover, *iD* is the first point of the *ith* order where *D = M*, and then the segments do not overlap. However, *D = M/2*, 50 % overlapping occurs between the consecutive data segments. After that, each data segment was windowed to obtain the overall PSD. The Eq.2.5. represents the modified periodogram:

$$\bar{P}_X^{(i)}(f) = \frac{1}{MU}\left|\sum_{n=0}^{N-1} x(n)w(n)e^{-j2\pi fn}\right|^2 \quad (\mathbf{2.5})$$

where *U* is the normalization factor in the window function of power ''*w(n)*'' as:

$$U = \frac{1}{M}\sum_{n=0}^{N-1} w^2(n) \quad (\mathbf{2.6})$$

The references can be examined for more details of PSD and Welch's method [8]. In our research, eight segments and 50% overlapping with hamming windows were used for data samples.

The collected data set for each subject have (6×8×1024)×19 dimension that 1024 stands for sampling frequency, 8 means total durations for four right and four left tongue motions in a trial, six presents 6 s of contact duration for discrete tongue movements and 19 are the channel numbers. Throughout the feature extraction, 100 ms was applied to form the feature vector due to the covering all EEG frequencies. 1 second data have 1024/100ms=10 parts (approx), therefore (6x8x10) equals 480 data length. However, some of the subjects were not able to start and end the sessions at the exact time during the experiment. For this reason, we have to cut out and equalize the data set for each trial and participant to 400 data lengths. Finally, the raw data set was set to 400x19 for each subject.

2.3. Principal Component Analysis

Principal component analysis (PCA) constructs a set of new orthogonal features by calculating the data variance, called principal components. PCA intends to take away the unnecessary data. Thus, easier computation is obtained for MLs [8]. Calculating the eigenvalues and eigenvectors of the covariance matrix (*C*) are employed in converting higher dimensional vector (X_t) into a lower dimensional one (S_t). The concerned equations of PCA are those:

$$C(X) = \sum_{1}^{N} \frac{(X_i X^T)}{N} \quad (\mathbf{2.7})$$

$$\lambda_i u_i = Cu_i, \qquad i = 1,2,3 \dots m \quad (\mathbf{2.8})$$

where λ_i presents the eigenvalues and u_i is named as the corresponding eigenvector of covariance matrix.

$$S_t(i) = u_t^T X_t, \qquad i = 1,2,3 \dots m \quad (\mathbf{2.9})$$

where $S_t(i)$ defines the principal components of the (X_t) [8]. By selection of principal components according to the variance values, In this research, twelve features' vector were created for a 400×12 data set indicating in the range of 98.18%-99.79%. The feature selection process by PCA and ICA was shown in Fig.3.

Figure 3. Feature selection process (PCA and ICA).

2.4. Independent Component Analysis

Independent component analysis (ICA) is a very powerful method for revealing concealed factors called independent components. ICA is a kind of statistical technique aiming to find linear projections of data that maximize mutual independence. Also, the widespread blind source separation (BSS) technique is based on ICA that can be used to select the best EEG channels. The system of assistive technologies with fewer EEG channels is preferred for better portability and convenience. In particular, ICA may serve to understand the functioning of the human brain easier as a finer mapping of brain responses during voluntary tongue movements [13].

$$x_i(t) = a_{i1}s_1(t) + \cdots + a_{in}s_n(t) \quad i = 1,2,\dots,n \quad (\mathbf{2.10})$$

where x_i *(t)* is the linear signal mixture belongs to *n* differently and randomly varying coefficients, and s_n *(t)* is the hidden component [8], as shown in Eqs.2.10-2.12. ICA notation can be presented in matrix form below:

Celal Bayar University Journal of Science
Volume 16, Issue 1, 2020, p 35-46
Doi: 10.18466/cbayarfbe.571994

$$\begin{bmatrix} x_1(t) \\ \vdots \\ x_n(t) \end{bmatrix} = A \begin{bmatrix} s_1(t) \\ \vdots \\ s_n(t) \end{bmatrix}, \quad A = [a_{i1}, a_{i2}, \dots, a_{in}] \quad (\mathbf{2.11})$$

$$x = As \quad (\mathbf{2.12})$$

In this article, ICA was employed to reduce the size of the data (400×12) for the (400×19) raw data set, and the results compared to PCA.

3. Machine Learning Algorithms

Applying feature extraction and feature selection (PCA-ICA) operations, the data set is conveyed to classifiers to discriminate glossokinetic potential responses for 1-D movements. Support vector machine and linear discriminant analysis are the common pattern recognition algorithms in biomedical signal processing and called kernel-based methods adapting the problem easier [8].

Accuracy (ACC), specificity (SPEC), sensitivity (SENS), and information transfer rate (ITR) was calculated to evaluate the performance of the GKP-based TMI. All the results were processed using the k-fold cross-validation technique, which is called the hold-out method to take out one part of the k-divided parts and structure the training data set. Moreover, the rest of the (k-1) parts are joined to form the test data set. Then all processes are repeated k-times in the independence of selection for samples [8]. In this study, 10-fold cross-validation was employed on all processed results for more robustness. Mathematical equations for the accuracy of the classification success can be seen in Eqs.3.1.-3.3.:

$$ACC(TS) = \frac{\sum_{i=1}^{|TS|} estimate(n_i)}{|TS|}, \; n_i \in TS \quad (\mathbf{3.1})$$

$$Estimate(n) = \begin{cases} 1, & if\ estimate(n) = cn \\ 0, & otherwise \end{cases} \quad (\mathbf{3.2})$$

$$Class.ACC = \frac{\sum_{i=1}^{|k|} accuracy(TS_i)}{|k|} \quad (\mathbf{3.3})$$

in which *TS* is the test data set, while $n \in TS$, c_n means the class of *n*. Furthermore, *estimate(n)* stands for the classification result of *n*, *k* is the number of k-fold cross validation [8].

Transmitting data of information per trial or time in EEG-based BCI systems is provided by information transfer rate (ITR). The ITR was produced from Shannon and Weaver's study and denoted by *B*. The approach of ITR can be seen in Eq.3.4.:

$$B = \log_2 N + P \log_2 P + (1-P) \log_2 \frac{(1-P)}{(N-1)} \quad (\mathbf{3.4})$$

B defines the bit numbers per trial, *N* is the different type of mental tasks, and *P* means the classification accuracy. The more various mental functions for a BCI system enhance the ITR, and the parameter value is shown in the range of (0-1) [8].

3.1. Support Vector Machine

Support vector machine is included in machine learning algorithm concept [8]. Support vectors are the keys for SVM to define the decision boundary (hyperplane). Margin is called as the distance from the hyperplane to the nearest support vectors for both sides. Then gaining generalization ability is aimed to maximize the margin and to find the optimal hyperplane [8], as depicted in Fig.4. The formulations of SVM is exhibited in Eqs.3.5-3.7.

$$X\{t\} = \begin{cases} r^t = +1, & x^t \in C1 \\ r^t = -1, & x^t \in C2 \end{cases} \quad (\mathbf{3.5})$$

$$g(x) = \begin{cases} w^T x^t + w_0 \geq +1, & x^t \in C1 \\ w^T x^t + w_0 \leq -1, & x^t \in C2 \end{cases} \quad (\mathbf{3.6})$$

$$r^t (w^T x^t + w_0) \geq +1 \quad (\mathbf{3.7})$$

The hyperplane is described by *g(x)*, w_0 situates the hyperplane and the orientation is pointed by *w*. Learning rate, initializations and checking for convergence is not carried out by SVM [8].

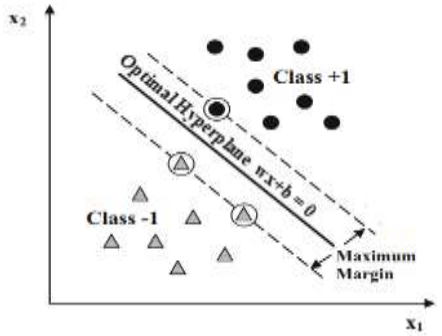

Figure 4. SVM and maximizing margin [8].

3.2. Linear Discriminant Analysis

Linear discriminant analysis is a kind of projection technique classifier reducing the dimension of the data. LDA intends to maximizing the between-class distance and minimizes within-class distance [22]. When *C1* and *C2* are the classes of the samples and LDA finds the projection direction (*w*) to discriminate the spatial pattern for maximum separability as possible. Formulations of LDA can be seen in Eqs.3.8-3.10.

$$z = w^T x \quad (\mathbf{3.8})$$

where, *x* (samples) are projected onto w. Projection technique of LDA is shown in Fig.5 below:

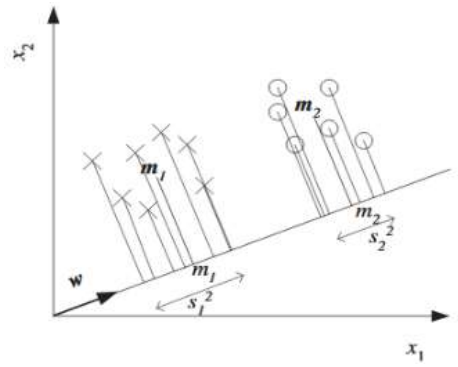

Figure 5. Classification task of LDA via the projection of data [8].

where projection technique implements from $\boldsymbol{m1}$ to $m1$ referring to means of samples in $C1$ before and after respectively. Thus, $\boldsymbol{m1} \in \Re^d$and $m1 \in \Re$. Then $\boldsymbol{m2}$ and $m2$ have the same means. s_1^2 and s_2^2 are scattered samples around the means [8]. If training sample is $X\{x^t, r^t\}$:

$$X\{t\} = \begin{cases} r^t = 1, & x^t \in C1 \\ r^t = 0, & x^t \in C2 \end{cases} \quad (\mathbf{3.9})$$

$$J(w) = \frac{w^T S_B w}{w^T S_W w} = \frac{|w^T(m1 - m2)|^2}{w^T S_W w} \quad (\mathbf{3.10})$$

where in $J(w)$, S_B and S_W are named as between-class scatter matrix and within-class scatter matrix, respectively. Moreover, *x* represents the input, *r* is the output in the training sample pairs.

4. Results

In this research, the discrimination of glossokinetic potential responses generated by the tongue for 1-D extraction has been investigated by implementing the SVM and LDA algorithms.

The mean-absolute value and power spectral density methods have been applied to machine learning methods. The raw data set for each participant was determined as a 400x19 dimension. The data sets to be processed by machine learning algorithms were obtained as:

- The raw data set (400x19)
- The data set reduced by PCA (400x12)
- The data set reduced by ICA (400x12)
- The frontal and temporal lobes' data set (11 channels) (400x11)

The classification performances were arranged according to the data sets above. All results throughout the article were represented in the decimal base and percentage expression (in %) except the outcomes of ITR. Then, the best and worst participants were stated by taking into account of results of the raw data set for distinguishing and comparison in an easy manner. Thus, the statements and implications of findings were stated on these subjects throughout the paper.

Table 3. Performance outcomes in the raw data set (400×19).

Met	..	Sb1	Sb2	Sb3	Sb4	Sb5	Sb6	Sb7	Sb8	Sb9	Sb10	Aver
LDA (MAV)	**Acc**	75.13	96.02	77.21	77.44	91.06	95.01	86.29	72.17	76.02	96.01	84.24
	Sen	76.52	93.50	79.98	73.13	90.80	97.05	84.00	64.19	68.88	97.83	82.59
	Spe	73.63	98.52	73.44	83.84	91.67	92.04	88.93	82.22	85.85	93.51	86.36
	ITR	0.191	0.759	0.226	0.230	0.565	0.714	0.423	0.147	0.205	0.758	0.422
LDA (PSD)	**Acc**	74.04	93.01	76.02	78.01	89.35	95.09	83.03	72.21	73.19	93.14	82.71
	Sen	72.23	88.50	76.98	71.47	91.21	97.46	76.60	63.32	59.73	97.83	79.53
	Spe	76.46	97.52	75.07	87.27	86.97	91.74	90.66	83.52	91.27	87.10	86.76
	ITR	0.174	0.634	0.205	0.240	0.511	0.717	0.343	0.147	0.161	0.640	0.377
SVM (MAV)	**Acc**	77.07	**97.03**	77.14	79.05	91.12	94.23	85.39	74.22	78.00	96.02	**84.93**
	Sen	87.23	97.50	84.55	80.49	93.33	96.20	83.59	69.21	74.02	97.84	86.4
	Spe	63.35	96.52	67.51	76.95	87.79	91.48	87.38	80.73	83.30	93.58	82.86
	ITR	0.223	0.807	0.224	0.259	0.567	0.682	0.400	0.177	0.240	0.758	0.434
SVM (PSD)	**Acc**	77.10	96.02	77.07	79.13	90.07	94.07	85.69	**67.80**	75.17	96.22	83.83
	Sen	86.40	96.00	82.71	73.55	92.45	97.03	80.22	85.77	62.77	99.13	85.6
	Spe	65.31	96.06	69.61	86.78	86.06	90.02	91.89	44.61	92.47	92.20	81.5
	ITR	0.224	0.758	0.223	0.261	0.533	0.675	0.408	0.094	0.191	0.768	0.414

Table 4. Performance outcomes in the PCA data set (400×12).

Met	..	Sb1	Sb2	Sb3	Sb4	Sb5	Sb6	Sb7	Sb8	Sb9	Sb10	Aver
LDA (MAV)	Acc	77.26	95	79.07	75.18	89.16	94.04	84.7	69.02	71	94.04	82.85
	Sen	79.29	91	81.38	73.59	88.64	96.2	81.26	61.05	60.13	95.71	80.82
	Spe	74.41	99.02	76.57	77.33	90.02	91.17	88.65	78.94	86.01	91.48	85.36
	ITR	0.226	0.714	0.26	0.192	0.505	0.674	0.383	0.107	0.131	0.674	0.387
LDA (PSD)	Acc	75.12	91.29	78.1	76.05	87.31	91.15	82.25	66.01	67.02	93.02	80.73
	Sen	71.25	85	80.51	73.19	89.51	93.7	69.94	69.8	48.53	96.96	77.84
	Spe	80.24	97.49	75.03	79.78	84.03	87.82	96.25	61.33	92.44	87.49	84.19
	ITR	0.191	0.573	0.242	0.206	0.451	0.568	0.325	0.075	0.085	0.635	0.335
SVM (MAV)	Acc	77.03	**97.01**	77.16	76.39	91.04	95.24	85.31	**69.05**	72.01	95.07	**83.53**
	Sen	85.85	97.5	82.79	81.43	91.65	96.61	82.71	65.65	61.9	97.83	84.39
	Spe	65.55	96.43	69.89	69.41	89.94	93.13	88.09	73.06	85.74	91.5	82.27
	ITR	0.223	0.806	0.225	0.211	0.565	0.724	0.398	0.107	0.145	0.717	0.412
SVM (PSD)	Acc	79.33	95.02	76.33	77.62	88.16	93.01	84.1	61.13	68.28	95.01	81.8
	Sen	86.78	95	86.26	79.2	90.82	96.56	77.47	87.53	55.43	97.84	85.29
	Spe	70.02	95.09	63.65	75.67	84.59	88.01	91.65	27.41	86.04	91.31	77.34
	ITR	0.265	0.715	0.21	0.233	0.475	0.634	0.368	0.036	0.099	0.714	0.375

The highest accuracy of the classification performance in the raw data set (400x19-Table 3) was obtained as 97.03% in SVM+MAV method. Then the lowest result was achieved with SVM+PSD method as 67.80%. Thus, Subject-2 (the best subject) and Subject-8 (the worst subject) were defined as the highlighted participants in the article. The accuracy results are very close to each other except for LDA+PSD (93.01%) in the best subject. After that, the LDA+MAV and SVM+PSD values were calculated as the same (96.02%). However, the SENS, SPEC, and ITR values are different. For the worst subject, SVM+MAV had the highest score (74.22%), followed by LDA+PSD and LDA+MAV as 72.21% and 72.17% success, respectively. The similarity was observed for the highest average result with SVM+MAV (84.93%).

Reduced data set with PCA (400×12) has relatively successful results represented in Table 4. The SVM+MAV method provided the highest outcomes for the best (97.01%) and worst (69.05%) participants. Then SVM + PSD (95.02%), LDA+MAV (95.00%), and LDA + PSD (91.29%) were achieved in terms of accuracy for the best subject. Meanwhile, the worst subject's results were ranked in decreasing order as LDA+MAV (69.02%), LDA+PSD (66.01%), and SVM+PSD (61.13%). Similar to the highest value of raw data set results, SVM+MAV was characterized by 83.53%. Hence consistent result (1.64% decreasing) was obtained compared to the average highest value of the raw data set (84.93%). The presentation of the covariance matrix for reduced data set was exhibited between the 98.18%-99.79% values. And the average highest presentation was observed as 99.45% with PSD.

According to Table 5, ICA results seem to be better than PCA [8]. Especially, the worst subject has reached 74.03% (in SVM+MAV), an increasing percentage is 6.72 (compared to 69.05%). Moreover, the other MLs also have greater outcomes compared to the PCA for the worst subject. On the other hand, the variations for the best subject is limited, and the results are close to the PCA. The best participant achieved 96.28% accuracy (in SVM+MAV), and the decline is about 0.75% compared to the highest outcome of PCA (97.01%). Moreover, the ultimate mean accuracy is again provided by SVM+MAV method (84.35%), and 0.97% boosting was obtained to the PCA.

The brain is structured by different functional lobes consisting of the cerebral and subcortical regions. Core and crucial functions of the body, such as involuntary breathing and heartbeat, are implemented by subcortical neuronal areas. Then the brain cortex carries out high-level functions such as conscious thinking and planning related to the voluntary movement of body functions, including tongue movement. The frontal lobe is known in charge of attention, planning, conscious motor functions, and behavioral control. Then, the temporal lobe is known in language-speech and face recognition as well as in the responsible of memory [8]. Thus voluntary tongue movement needs focus and planning efforts in fast, rhythmic, and stable motions during GKP-based TMI experimental work. For this reason, the results of frontal and temporal lobes were observed against voluntary tongue movements.

One of the goals of the GKP-based TMI is to explain the effect and contribution of different lobes of the brain

to the tongue-machine interface in terms of the classification accuracy. Therefore, the data set of 400×11 were generated by extracting 11-channels (Frontal + Temporal Lobe) data sets from the raw data set (400×19). T3, T4, T5, and T6 electrodes were used for eleven channels (Frontal + Temporal Lobe) as well as these seven electrodes for the seven channels (Fp1, Fp2, F7, F8, Fz, F3, and F4) (Frontal Lobe), as shown in Table 1.

According to Table 6, the joining effect of the frontal and temporal lobes for GKP-based TMI are encouraging and robustness compared to the raw data set (400×19) results. Not only the individual's success is observed highly acceptable, but also average achievements are in similar conditions. The best subject had provided 97.05% accuracy via SVM+MAV when the worst subject realized 71.06% correctness with the LDA+MAV algorithm. The deviation for the best and worst participant have increasing (0.02%) and decreasing (4.25%) characteristic respectively. Again the greatest outcome of average accuracy is observed in SVM+MAV (83.22%). The boosting impact of the temporal lobe (11-channels) to the frontal lobe (7-channels) was obtained as a 6.37% value. Thus, the performance of eleven channels seems to be more accurate and consistent outcomes than seven channels. It's almost as good as 19-channels of success. During experimental tasks, GKP signal variations for concentrated participants occur in the delta and theta bands [3]. The discriminating power of each tongue movements touching the buccal walls has spatial patterns on the scalp. As shown in Figs.6 and 7, to further analyze the brain mappings of the best subject, the high power alterations can be observed on the frontal and temporal lobe regions and partly pre-motor and motor cortex on delta bands. This vital finding was confirmed by the classification success shown in Table 6. Moreover, in theta and alpha frequency bands, negligible power assessments were obtained to distinguish the certain GKP responses. However, insufficient power signals were occurred at the occipital lobe between the beta frequency bands on the co ntralateral hemispherical side of the brain, depending on the visual stimulus in front of the LCD monitor [8].

The brain mappings for the worst participant (Figs. 8 and 9) showed dissimilar characteristics as against to the best subject. First, there are high-intensity power signal variations in the frontal lobe, but not lying correctly and smoothly in the temporal lobes of the delta and theta frequency. However, the temporal lobe power signal variations of the best subject include the T3, T4, T5, and T6 electrode locations shown in Fig.6 and Fig.7. Another crucial distinction in the worst subject is that the theta frequencies have highly acceptable power signals on the frontal lobe, which includes only Fp1 and Fp2. Furthermore, parietal lobe power signals are higher than the best subject's own. The reason for this may be that the worst subject was to deal with experimental tasks with inadequate target-oriented motivation and disturbing perception [8].

Table 5. Performance outcomes in the ICA data set (400×12).

Met	..	Sb1	Sb2	Sb3	Sb4	Sb5	Sb6	Sb7	Sb8	Sb9	Sb10	Aver
LDA (MAV)	**Acc**	76.13	93.05	78.45	77.42	88.82	94.22	87.01	73.44	75.53	95.51	83.96
	Sen	78.81	89.5	81.88	73.19	89.15	95.4	86.36	67.33	65.89	97.84	82.54
	Spe	72.14	96.64	74.47	83.01	88.34	92.41	87.65	81.19	89	92.42	85.73
	ITR	0.207	0.636	0.248	0.229	0.495	0.681	0.443	0.165	0.197	0.736	0.404
LDA (PSD)	**Acc**	75.15	92.5	76.05	78.65	89.12	93.27	82.38	73.05	73.18	93.19	82.65
	Sen	73.56	88.5	79.9	72.68	92.01	94.51	81.19	64.78	61.03	97.83	80.6
	Spe	76.66	96.52	70.63	86.19	84.74	91.5	83.39	83.52	89.76	86.61	84.95
	ITR	0.191	0.616	0.206	0.252	0.504	0.644	0.328	0.159	0.161	0.641	0.37
SVM (MAV)	**Acc**	77.01	**96.28**	77.29	79.23	90	93.06	85.25	**74.03**	77.33	94.01	**84.35**
	Sen	85.06	96	83.52	80.14	90.8	94.13	82.23	70.04	74.02	95.24	85.12
	Spe	66.41	96.39	68.79	78.65	88.78	91.68	88.53	79.01	82.21	92.19	83.26
	ITR	0.222	0.771	0.227	0.263	0.531	0.636	0.397	0.174	0.228	0.673	0.412
SVM (PSD)	**Acc**	76.89	95.24	77.02	80.24	88.17	94.59	83.15	73.01	76.05	95.77	84.01
	Sen	88.18	96	85.32	78.3	93.7	97.01	80.74	66.92	67.12	97.83	85.11
	Spe	62.21	94.39	66.19	83.4	80.3	91.19	85.97	80.97	88.33	93.17	82.61
	ITR	0.22	0.724	0.222	0.283	0.476	0.696	0.346	0.159	0.206	0.747	0.408

Table 6. Performance outcomes in the 11-channels (Frontal Lobe+Temporal Lobe) data set (400×11).

Met	..	Sb1	Sb2	Sb3	Sb4	Sb5	Sb6	Sb7	Sb8	Sb9	Sb10	Aver
LDA (MAV)	Acc	76.08	96.25	76.2	72.06	88.03	94.26	87.16	**71.06**	72.07	94.02	82.72
	Sen	76.17	94	80.45	70.14	89.53	95.76	83.96	62.96	61.01	96.54	81.05
	Spe	76.11	98.55	70.19	74.12	85.64	91.87	90.88	81.66	87.14	90.49	84.66
	ITR	0.206	0.769	0.208	0.145	0.472	0.683	0.447	0.132	0.145	0.673	0.388
LDA (PSD)	Acc	76.3	92	77.04	69.12	87.23	92.05	83.04	69.4	68.03	92.08	80.63
	Sen	75.36	87.5	82.67	64.06	89.55	95.76	72.32	71.01	50.69	97.39	78.63
	Spe	77.3	96.37	70.49	76.12	83.59	86.95	95.44	67.38	91.52	84.75	82.99
	ITR	0.21	0.598	0.223	0.108	0.449	0.6	0.343	0.111	0.096	0.6	0.334
SVM (MAV)	Acc	79.14	**97.05**	75.27	72.03	88.29	94.29	86.02	70.06	74.07	96.01	**83.22**
	Sen	88.52	97.5	83.14	75.78	90.4	96.21	83.98	70.45	66.65	99.57	85.22
	Spe	67.08	96.54	64.95	66.52	85.14	91.42	88.23	69.65	84.13	91.11	80.48
	ITR	0.261	0.808	0.193	0.145	0.479	0.684	0.416	0.119	0.174	0.758	0.404
SVM (PSD)	Acc	79.46	95.02	72.41	71.2	89.06	93.22	84.25	62.2	70.01	94.01	81.08
	Sen	89.33	95	87.61	72.3	92.9	96.2	75.17	91.92	54.09	96.96	85.15
	Spe	66.57	94.94	53.43	70.03	83.08	88.12	94.59	24.19	91.86	89.81	75.66
	ITR	0.267	0.714	0.15	0.134	0.502	0.642	0.372	0.043	0.119	0.673	0.362

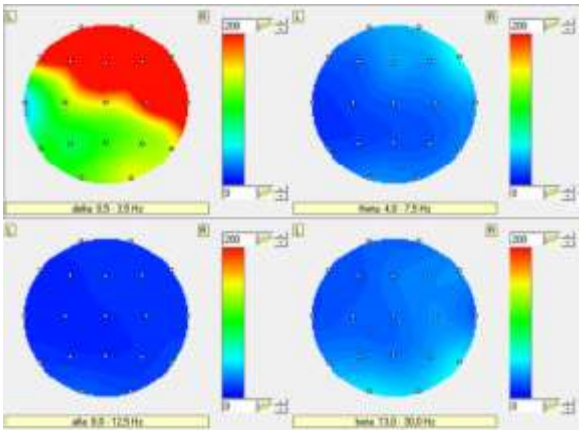

Figure 6. The best participant's brain mapping in touching the right buccal wall (delta, theta, alfa, beta frequencies).

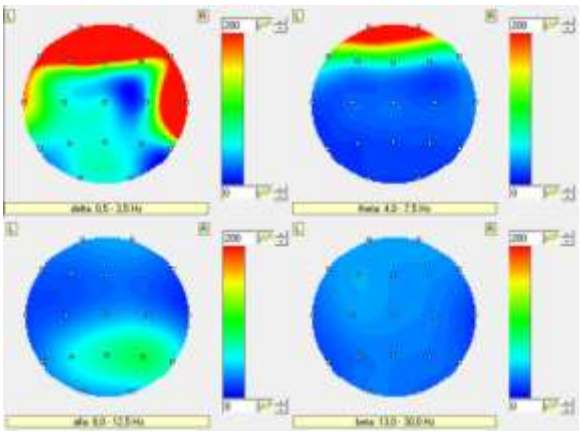

Figure 8. The worst participant's brain mapping in touching the right buccal wall (delta, theta, alfa, beta frequencies).

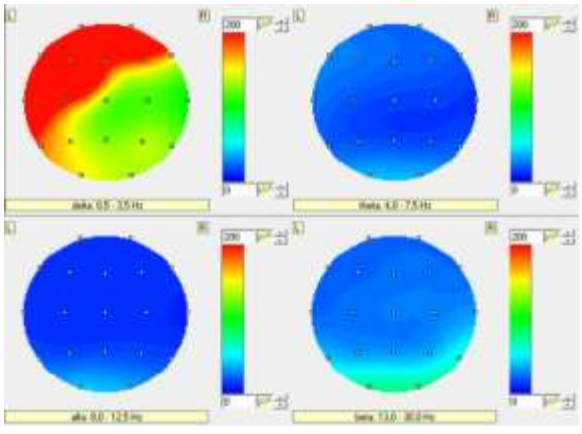

Figure 7. The best participant's brain mapping in touching the left buccal wall (delta, theta, alfa, beta frequencies).

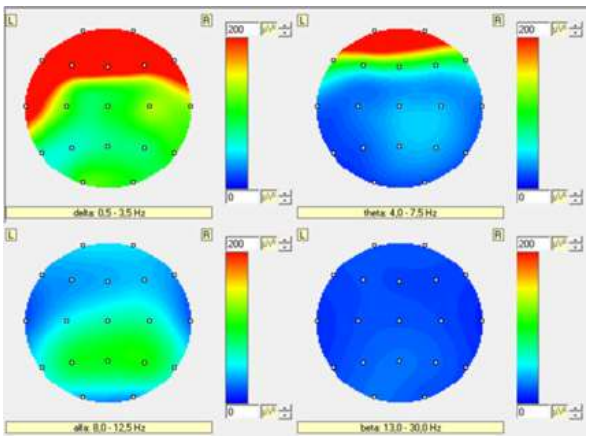

Figure 9. The worst participant's brain mapping in touching the left buccal wall (delta, theta, alfa, beta frequencies).

Table 7. Computation times of the linear discrimant analysis and support vector machine process.

Method	LDA +MAV	LDA +PSD	SVM +MAV	SVM +PSD
F.E.T.+ C.T.	0.0057	0.9222	0.0028	0.8936

F.E.T. (Feature Extraction Time-s), C.T. (Classifying Time-s)

The computation time is a significant metric for TMI's real-time applications [1, 5]. According to Table 7, the SVM+MAV method is shown the least computation time (0.0028 s) among the other methods. Then LDA+MAV (0.0057 s) yielded faster performance than SVM+PSD (0.8936 s) and LDA+PSD (0.9222 s) methods. It can be observed that the mean-absolute value has less computation time than the power spectral density because of not requiring transformation from the time domain to the frequency domain [8]. Similarly, SVM has less processing time than LDA. Computation time results were acquired in 1-fold cross-validation for an average of the test samples in the best participant's raw data set. All reported results in this paper were realized using MATLAB (License No: 834260) on a computer (Intel Core i5-7200 U CPU 2.50 GHz, Windows 10, 64 bit and 8 GB RAM). Finally, it is noteworthy that the SVM+MAV method is the best algorithm concerning the classification accuracy and the speed of execution in real-time usage of the GKP-based TMI research. Furthermore, the MAV feature extraction method provided better outcomes than PSD regarding the average values. Perhaps because of this reason, the MAV feature reflects the proper representation of glossokinetic potential responses better in GKP-based TMI.

5. Discussion

Computational neuroscience information notices the design of feedback control methods to distinguish the area of the motor cortex at different electrode installations on the human-computer interfaces during activated human body parts by measuring the local field potentials (LFPs). Thus, the multidisciplinary investigation aims to design a modern brain-machine interface (BMI) reconciling the statistical signal processing, machine learning, and information theory [15]. It is worth to report that the contribution and effects of the frontal+temporal lobes (11-channel) were observed in Tables 6, respectively. The correlation of frontal and temporal lobes' results are highly promising in terms of the classification accuracy for the tongue motion. Therefore, the results of eleven-channels are very close to the raw data set's (400×19) outcomes. This significant finding was also verified by the brain mappings of the best participant shown in Figs.6 and 7. Moreover, fewer electrodes with 11-channels may provide more degrees of freedom and reliable control to the GKP-based TMI [9-10]. For this reason, fewer electrodes can lead "wearable" and easy-to-use biomedical support technologies and ATs to work in the future for stroke individuals [17]. Moreover, corticomuscular coupling analysis reveals the mutual effect amid ongoing muscular activities (EMG) and the brain regions. However, the brain cortex and GKP coherence in delta and theta bands during the tongue-muscle motor functions were realized by GKP-based TMI research for the first time in the literature as our best knowledge.

The unexpected case of the study of Nam et al. is that the antisymmetric formation of GKP responses has emerged on the power of brain mapping. However, in our research, the power of GKP responses on the brain mappings has arisen in symmetric creation. This may have occurred from this reason; in the case of producing GKP signals, the same team noted that the negatively charged of the tip of the tongue uncover a potentially increased variation on the noncontact surface as it creates a negative potential reduction on the contact surface of the buccal wall [3-5]. On the other hand, Nam et al. have investigated the patterns of GKPs on the scalp related to the language and phonetics research.

The GKP biological responses are constituted of different spatial and temporal patterns on the brain maps during tongue movement. Moreover, in the mentioned paper, pronouncing the retroflex consonants led to a very strong potential increase over the frontal lobe during the tongue bending [14]. For this reason, in our study, an antisymmetric occurrence may have been suppressed due to strong and fast movements while the tongue is bent to touch the buccal walls during experimental tasks. Therefore, our results may have a symmetrical formation on the brain maps, as shown in Figs.7 and 8. The same researchers noted that the electrode location and the reference point, which was intentionally taken different contrary to general manner to occur the antisymmetric state on the brain mappings. Also, the experimental setup is different compared to our work, not just unlike electrode configurations. In their study, the tongue moves in an uninterrupted motion on the right-front-left path to touch the buccal walls [4-5]. However, in our study, multiple discrete contacts were realized in the same duration of 6 s task. Thus, all these points might encourage the assumption of symmetrical outcomes on brain maps in our study.

The results of GKP-based TMI may be considered more reliable and robust, depending on 8 male and 2 female subjects (all naive healthy) who were not previously experienced. Then, Subject_2 (the best subject) and Subject_8 (the worst subject) were chosen to point out and compare the distinct spots. The distinctive distinction of the best participant shows that having motivation, distinct and fast tongue movements provides the basis of achievement. However, the success of the worst participant was acceptable because

of less concentration and not properly doing instructed tasks. Motivation and cognitive effort in the relevant literature have been identified as the critical parameter for the high performance of BCI / HMI [8].

In recent years, ICA has been widely utilized in EEG-based BCI models to reduce the dimension of features or to reveal the source components. However, it has not been used in GKP signals to reveal the sources and reduce the dimension. Therefore, when these two methods are used, both ends of the predictions about the statistical distribution of the data are tried. Not all EEG signals are non-Gaussian (ICA) and uncorrelated (PCA). This basis may be the same for GKP signals. Therefore, according to Tables 4 and 5, PCA and ICA results are so close to each other. However, ICA is relatively better than PCA, especially for the worst and low participants. Because of this reason may be that the data set of the worst subject has more non-Gaussian and highly spatial overlapping of cortical activity [18]. Moreover, finding linear projections of the data by ICA aims is to maximize their mutual independence. Therefore, the selection process of the 12 EEG channels was made to maximize the classification results in the randomly searching algorithm for each iteration [8, 18]. The advantages and disadvantages for ICA and PCA were stated in Table 8:

Table 8. ICA and PCA comparison for data sets.

ICA	PCA
ICA can improve classifier performance as it moves away from the normal distribution (non-Gaussian). Therefore, the insignificant and worst participant data sets are more fitting for ICA	PCA is benefiting from the normal distribution of data. Thus, better participant performances can be improved by PCA
More convenient for highly spatial overlapping of cortical activity. Therefore, EEG channels from different parts of regions can be separated by ICA. However, the selection process can take a long time	New orthogonal features, called principal components, are calculated by PCA. Thus, dimension reduction and selection of high variance features are easy to compute. However, PCA is not enough to resolve complex brain signals
Removal artifact of signals can be made by ICA	Focusing on the reduction of data and decreasing the classification cost time

In BCIs, inter-trial and inter-subject instability are observed an important problem regarding the performance and reliability of the system. Moreover, long sessions of the BCI process present challenges in terms of consistent classification. The concept of these issues is referred to as transfer learning techniques that describe a procedure for using a stored relative data (statistical distribution of trial or session) to improve performance in another task [15]. However, the GKP-based TMI study may offer greater robustness for trial effects due to the voluntary tongue movements and glossokinetic potential responses with high amplitude and low frequencies [3, 4].

Moreover, it has been reported that the flexible and long cognitive planning time experiments can advance to the BCI and HMI research due to goal-oriented results that allow the subject to instinctive considerations [8]. In future work, the GKP-based TMI system can be advanced over this concept.

6. Conclusion

This paper describes GKP-based TMI as a new 1-D tongue machine interface research applying mean-absolute value and power spectral density methods with SVM and LDA over scalp-recorded GKP biosignals. Some of the equipment based tongue-machine interfaces have reached up to the 96-98% accuracy [12]. However, these systems have bulky devices inside the mouth and in the ear canal or around the headset for stroke people.

The rarely used glossokinetic responses have given promising results reaching up to the 97.03 accuracies for the construction of assistive technology that can be natural, reliable, attractive, and high-throughput efficiency for locked-in and ALS conditions. Then frontal and temporal lobe contributions can help neuroscientific understanding of cortical activity and statistical signal processing techniques by measuring local field potentials (LFPs) for tongue-related motor functions [16]. As far as we know, this critical point and glossokinetic potential have been dealt for the first time regarding the classification success of SVM and LDA with mean-absolute value and power spectral density in a tongue-machine interface. Moreover, comparing to our previous articles, SVM and LDA algorithms using mean-absolute value has greater performances compared to the root-mean-square feature extraction method for the best subject. Then this outcome provides very close results to the neural networks in the raw data sets [19-20].

The main challenges and focal point of this article are dedicated to advance the life quality of paralyzed individuals with tongue-based ways to reveal their wishes without traditional neuro-muscular pathways. Furthermore, GKP-based TMI may give a lead of real-time alternative control channels for traditional EEG-

driven BCIs with significant deficiencies resulting from the nature of EEG signals, which are low signal-to-noise ratio, and internally induced stationary mental activities or some external factors.

The future work of this research study can be progressed by real-time applications using wireless, highly accurate data acquisition devices with fewer electrodes for developing more portable systems. Moreover, the real-time system performances should be recorded on the different levels of paralyzed people.

Acknowledgement

The authors would like to thank Bozok University students for their participation in this research.

Author's Contributions

Kutlucan Gorur: Drafted and wrote the manuscript, performed the experiment, and result analysis. He also contributed to the main concept of the experiment.

M.Recep Bozkurt: Assisted in analytical analysis on the structure, supervised the experiment's progress, result interpretation.

M. Serdar Bascil: Helped in manuscript preparation and interpretation of the results.

Feyzullah Temurtas: Contributed to the theory and conceptual ideas.

Ethics

The study was confirmed by the Ethical Committee of Sakarya University (61923333/044). All procedures performed in studies involving human participants were in accordance with the ethical standards of the institutional and / or national research committee. Informed consent was obtained from all individual participants who participated in the study.

References

1. Huo, X, Ghovanloo, M. 2012. Tongue Drive: A wireless tongue-operated means for people with severe disabilities to communicate their intentions. *IEEE Communication Magazine*; 50(10):128-135.

2. Andreasen, Struijk, L.N.S. 2006. An inductive tongue computer interface for control of computers and assistive devices. *IEEE Transactions on Biomedical Engineering*; 53(12):2594-2597.

3. Nam, Y, Koo, B, Cichocki, A, Choi, S. 2016 Glossokinetic Potentials for a tongue–machine interface. *IEEE Systems, Man, & Cybernetics Magazine*; 2(1): 6-13.

4. Nam, Y, Zhao, Q, Cichocki, A, Choi, S. 2012. Tongue-Rudder: A Glossokinetic-Potential-Based tongue–machine interface. *IEEE Transactions on Biomedical Engineering*; 59(1): 290-299.

5. Nam, Y, Koo, B, Cichocki, A, Choi, S. 2014. GOM-Face: GKP, EOG, and EMG-Based multimodal interface with application to humanoid robot control. *IEEE Transactions on Biomedical Engineering*; 61(2):453-462.

6. Tang, H, Beebe, D.J. 2006. An oral tactile interface for blind navigation. *IEEE Transaction On Neural Systems & Rehabilitation Engineering*; 14(1):116-123.

7. Bao, X, Wang, J, Hu, J. Method of individual identification based on electroencephalogram analysis, International Conference on New Trends in Information and Service Science, 2009, pp 390-393.

8. Gorur, K. Makine Öğrenmesi Algoritmaları Kullanılarak Glossokinetik Potansiyel Tabanlı Dil-Makine Arayüzü Tasarımı; Sakarya Üniversitesi Fen Bilimleri Enstitüsü: Doktora Tezi, Sakarya, 2019.

9. Reuderink, B, Poel, M, Nijholt, A. 2011. The impact of loss of control on movement BCIs. *IEEE Transaction On Neural Systems & Rehabilitation Engineering*; 19(6):628-637.

10. Rupp, R, Rohm, M, Schneiders, M, Kreilinger, A, Müller-Putz, G.R. 2015. Functional rehabilitation of the paralyzed upper extremity after spinal cord injury by noninvasive hybrid neuroprostheses. *Proceedings of the IEEE*; 103(6):954-968.

11. Krishnamurthy, G, Ghovanloo, M. Tongue Drive: A tongue operated magnetic sensor based wireless assistive technology for people with severe disabilities, IEEE International Symposium on Circuits and Systems, 2006, pp 5551-5554.

12. Vaidyanathan, R, Chung, B, Gupta, L, Kook, H, Kota, S., West, J.D. 2007. Tongue-movement communication and control concept for hands-free human–machine interfaces. *IEEE Systems, Man, & Cybernetics Magazine*; 37(4):533-546.

13. Vigário, R, Särelä, J, Jousmäki, V, Hämäläinen, M., Oja, E. 2000. Independent component approach to the analysis of EEG and MEG recordings. IEEE Transactions on Biomedical Engineering; 47(5):589-593.

14. Nam, Y, Bonkon, K, Choi, S. Language-related glossokinetic potentials on scalp, IEEE International conference on systems, Man, and Cybernetics, San Diego, USA, 2014, pp 1063-1067.

15. Jayaram, V, Alamgir, M, Altun, Y, Schölkopf, B, Grosse-Wentrup, M. 2016. Transfer learning in brain-computer interfaces. IEEE Computational Intelligence Magazine; 20-31.

16. Kao, J.C, Stavisky, S.D, Sussillo D, Nuyujukian, P, Shenoy K.V. 2014. Information systems opportunities in brain–machine interface decoders. Proceedings of the IEEE; 102(5):666-68.

17. Cerutti, S. 2009. In the Spotlight: Biomedical signal processing. IEEE Reviews In Biomedical Enginering; 2:9-11.

18. Genc, H.M, Cataltepe, Z, Pearson, T. A New PCA/ICA based feature selection method, IEEE Signal Processing and Communations Applications, Eskisehir, Turkey, 2007.

19. Gorur, K, Bozkurt M.R, Bascil M.S, Temurtas F. 2018. Glossokinetic potential based tongue–machine interface for 1-D extraction. Australasian Physical & Engineering Sciences in Medicine; 41(2):379-391.

20. Gorur K, Bozkurt M.R, Bascil M.S, Temurtas F. 2018. Glossokinetic potential based tongue–machine interface for 1-D extraction using neural networks, Biocybernetics and Biomedical Engineering; 38(3):745-759.